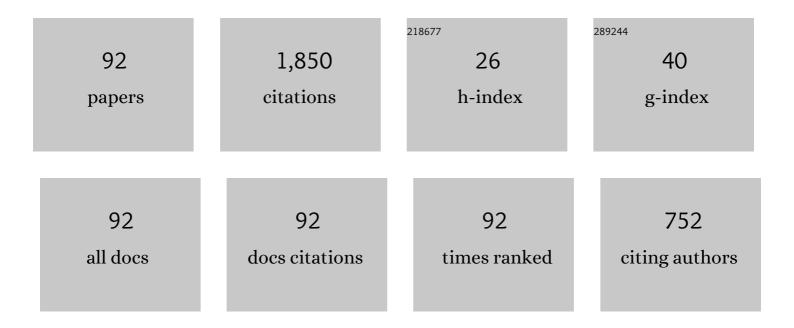
Guang-Cai Sun

List of Publications by Year in descending order

Source: https://exaly.com/author-pdf/5497851/publications.pdf Version: 2024-02-01



#	Article	IF	CITATIONS
1	Robust Ground Moving-Target Imaging Using Deramp–Keystone Processing. IEEE Transactions on Geoscience and Remote Sensing, 2013, 51, 966-982.	6.3	183
2	Focus Improvement of Highly Squinted Data Based on Azimuth Nonlinear Scaling. IEEE Transactions on Geoscience and Remote Sensing, 2011, 49, 2308-2322.	6.3	107
3	Motion Compensation/Autofocus in Airborne Synthetic Aperture Radar: A Review. IEEE Geoscience and Remote Sensing Magazine, 2022, 10, 185-206.	9.6	81
4	A 2-D Space-Variant Chirp Scaling Algorithm Based on the RCM Equalization and Subband Synthesis to Process Geosynchronous SAR Data. IEEE Transactions on Geoscience and Remote Sensing, 2014, 52, 4868-4880.	6.3	78
5	A Frequency-Domain Imaging Algorithm for Highly Squinted SAR Mounted on Maneuvering Platforms With Nonlinear Trajectory. IEEE Transactions on Geoscience and Remote Sensing, 2016, 54, 4023-4038.	6.3	72
6	Sliding Spotlight and TOPS SAR Data Processing Without Subaperture. IEEE Geoscience and Remote Sensing Letters, 2011, 8, 1036-1040.	3.1	64
7	A 2-D Space-Variant Motion Estimation and Compensation Method for Ultrahigh-Resolution Airborne Stepped-Frequency SAR With Long Integration Time. IEEE Transactions on Geoscience and Remote Sensing, 2017, 55, 6390-6401.	6.3	54
8	Acceleration Model Analyses and Imaging Algorithm for Highly Squinted Airborne Spotlight-Mode SAR with Maneuvers. IEEE Journal of Selected Topics in Applied Earth Observations and Remote Sensing, 2015, 8, 1120-1131.	4.9	49
9	Beam Steering SAR Data Processing by a Generalized PFA. IEEE Transactions on Geoscience and Remote Sensing, 2013, 51, 4366-4377.	6.3	43
10	Multichannel Full-Aperture Azimuth Processing for Beam Steering SAR. IEEE Transactions on Geoscience and Remote Sensing, 2013, 51, 4761-4778.	6.3	42
11	Processing of Very High Resolution Spaceborne Sliding Spotlight SAR Data Using Velocity Scaling. IEEE Transactions on Geoscience and Remote Sensing, 2016, 54, 1505-1518.	6.3	42
12	Terahertz Image Detection with the Improved Faster Region-Based Convolutional Neural Network. Sensors, 2018, 18, 2327.	3.8	42
13	Azimuth Resampling Processing for Highly Squinted Synthetic Aperture Radar Imaging With Several Modes. IEEE Transactions on Geoscience and Remote Sensing, 2014, 52, 4339-4352.	6.3	39
14	Two-Step Accuracy Improvement of Motion Compensation for Airborne SAR With Ultrahigh Resolution and Wide Swath. IEEE Transactions on Geoscience and Remote Sensing, 2019, 57, 7148-7160.	6.3	38
15	A Unified Focusing Algorithm for Several Modes of SAR Based on FrFT. IEEE Transactions on Geoscience and Remote Sensing, 2013, 51, 3139-3155.	6.3	37
16	Improved Signal Reconstruction Algorithm for Multichannel SAR Based on the Doppler Spectrum Estimation. IEEE Journal of Selected Topics in Applied Earth Observations and Remote Sensing, 2017, 10, 1425-1442.	4.9	36
17	Cartesian Factorized Backprojection Algorithm for High-Resolution Spotlight SAR Imaging. IEEE Sensors Journal, 2018, 18, 1160-1168.	4.7	36
18	Water Body Detection in High-Resolution SAR Images With Cascaded Fully-Convolutional Network and Variable Focal Loss. IEEE Transactions on Geoscience and Remote Sensing, 2021, 59, 316-332.	6.3	36

GUANG-CAI SUN

#	Article	IF	CITATIONS
19	Extended NCS Based on Method of Series Reversion for Imaging of Highly Squinted SAR. IEEE Geoscience and Remote Sensing Letters, 2011, 8, 446-450.	3.1	35
20	An Azimuth Frequency Non-Linear Chirp Scaling (FNCS) Algorithm for TOPS SAR Imaging With High Squint Angle. IEEE Journal of Selected Topics in Applied Earth Observations and Remote Sensing, 2014, 7, 213-221.	4.9	33
21	Simultaneous Stationary Scene Imaging and Ground Moving Target Indication for High-Resolution Wide-Swath SAR System. IEEE Transactions on Geoscience and Remote Sensing, 2016, 54, 4224-4239.	6.3	32
22	Ground Cartesian Back-Projection Algorithm for High Squint Diving TOPS SAR Imaging. IEEE Transactions on Geoscience and Remote Sensing, 2021, 59, 5812-5827.	6.3	30
23	Spaceborne Synthetic Aperture Radar Imaging Algorithms: An overview. IEEE Geoscience and Remote Sensing Magazine, 2022, 10, 161-184.	9.6	29
24	Deramp Space–Time Adaptive Processing for Multichannel SAR Systems. IEEE Geoscience and Remote Sensing Letters, 2014, 11, 1448-1452.	3.1	28
25	Squinted TOPS SAR Imaging Based on Modified Range Migration Algorithm and Spectral Analysis. IEEE Geoscience and Remote Sensing Letters, 2014, 11, 1707-1711.	3.1	27
26	A TSVD-NCS Algorithm in Range-Doppler Domain for Geosynchronous Synthetic Aperture Radar. IEEE Geoscience and Remote Sensing Letters, 2016, 13, 1631-1635.	3.1	27
27	Integration of Rotation Estimation and High-Order Compensation for Ultrahigh-Resolution Microwave Photonic ISAR Imagery. IEEE Transactions on Geoscience and Remote Sensing, 2021, 59, 2095-2115.	6.3	25
28	An Improved SAC Algorithm Based on the Range-Keystone Transform for Doppler Rate Estimation. IEEE Geoscience and Remote Sensing Letters, 2013, 10, 741-745.	3.1	24
29	A Real-Time Imaging Algorithm Based on Sub-Aperture CS-Dechirp for GF3-SAR Data. Sensors, 2018, 18, 2562.	3.8	24
30	A Modified CSA Based on Joint Time-Doppler Resampling for MEO SAR Stripmap Mode. IEEE Transactions on Geoscience and Remote Sensing, 2018, 56, 3573-3586.	6.3	21
31	A Parameter Optimization Model for Geosynchronous SAR Sensor in Aspects of Signal Bandwidth and Integration Time. IEEE Geoscience and Remote Sensing Letters, 2016, 13, 1374-1378.	3.1	20
32	Full-Aperture Focusing of Very High Resolution Spaceborne-Squinted Sliding Spotlight SAR Data. IEEE Transactions on Geoscience and Remote Sensing, 2017, 55, 3309-3321.	6.3	18
33	Focusing Improvement of Curved Trajectory Spaceborne SAR Based on Optimal LRWC Preprocessing and 2-D Singular Value Decomposition. IEEE Transactions on Geoscience and Remote Sensing, 2019, 57, 4246-4258.	6.3	18
34	An Analytical Resolution Evaluation Approach for Bistatic GEOSAR Based on Local Feature of Ambiguity Function. IEEE Transactions on Geoscience and Remote Sensing, 2018, 56, 2159-2169.	6.3	17
35	High-Speed Maneuvering Platforms Squint Beam-Steering SAR Imaging Without Subaperture. IEEE Transactions on Geoscience and Remote Sensing, 2019, 57, 6974-6985.	6.3	17
36	EFTL: Complex Convolutional Networks With Electromagnetic Feature Transfer Learning for SAR Target Recognition. IEEE Transactions on Geoscience and Remote Sensing, 2022, 60, 1-11.	6.3	17

Guang-Cai Sun

#	Article	IF	CITATIONS
37	A Two-Dimensional Beam-Steering Method to Simultaneously Consider Doppler Centroid and Ground Observation in GEOSAR. IEEE Journal of Selected Topics in Applied Earth Observations and Remote Sensing, 2017, 10, 161-167.	4.9	16
38	Focusing of Medium-Earth-Orbit SAR Using an ASE-Velocity Model Based on MOCO Principle. IEEE Transactions on Geoscience and Remote Sensing, 2018, 56, 3963-3975.	6.3	16
39	A Frequency Domain Backprojection Algorithm Based on Local Cartesian Coordinate and Subregion Range Migration Correction for High-Squint SAR Mounted on Maneuvering Platforms. IEEE Transactions on Geoscience and Remote Sensing, 2018, 56, 7086-7101.	6.3	16
40	Highly Squinted MEO SAR Focusing Based on Extended Omega-K Algorithm and Modified Joint Time and Doppler Resampling. IEEE Transactions on Geoscience and Remote Sensing, 2019, 57, 9188-9200.	6.3	16
41	Oriented Gaussian Function-Based Box Boundary-Aware Vectors for Oriented Ship Detection in Multiresolution SAR Imagery. IEEE Transactions on Geoscience and Remote Sensing, 2022, 60, 1-15.	6.3	15
42	Moving Target Refocusing Algorithm in 2-D Wavenumber Domain After BP Integral. IEEE Geoscience and Remote Sensing Letters, 2018, 15, 127-131.	3.1	14
43	A Novel Two-Step Approach of Error Estimation for Stepped-Frequency MIMO-SAR. IEEE Geoscience and Remote Sensing Letters, 2017, 14, 2290-2294.	3.1	13
44	A High-Squint TOPS SAR Imaging Algorithm for Maneuvering Platforms Based on Joint Time-Doppler Deramp Without Subaperture. IEEE Geoscience and Remote Sensing Letters, 2020, 17, 1899-1903.	3.1	13
45	2-D Frequency Autofocus for Squint Spotlight SAR Imaging With Extended Omega-K. IEEE Transactions on Geoscience and Remote Sensing, 2022, 60, 1-12.	6.3	11
46	A Channel Phase Error Correction Method Based on Joint Quality Function of GF-3 SAR Dual-Channel Images. Sensors, 2018, 18, 3131.	3.8	10
47	A New SAR–GMTI High-Accuracy Focusing and Relocation Method Using Instantaneous Interferometry. IEEE Transactions on Geoscience and Remote Sensing, 2016, 54, 5564-5577.	6.3	9
48	Clutter Suppression via Subspace Projection for Spaceborne HRWS Multichannel SAR System. IEEE Geoscience and Remote Sensing Letters, 2020, 17, 1538-1542.	3.1	9
49	High-Resolution Real-Time Imaging Processing for Spaceborne Spotlight SAR With Curved Orbit via Subaperture Coherent Superposition in Image Domain. IEEE Journal of Selected Topics in Applied Earth Observations and Remote Sensing, 2022, 15, 1992-2003.	4.9	9
50	Integrating the Reconstructed Scattering Center Feature Maps With Deep CNN Feature Maps for Automatic SAR Target Recognition. IEEE Geoscience and Remote Sensing Letters, 2022, 19, 1-5.	3.1	8
51	A Fast Cartesian Back-Projection Algorithm Based on Ground Surface Grid for GEO SAR Focusing. IEEE Transactions on Geoscience and Remote Sensing, 2022, 60, 1-14.	6.3	8
52	Improved focusing approach for highly squinted beam steering SAR. IET Radar, Sonar and Navigation, 2016, 10, 1394-1399.	1.8	7
53	Cartesian factorized backprojection algorithm for synthetic aperture radar. , 2016, , .		7
54	Performance Improvement and System Design of Geo-SAR Using the Yaw Steering. IEEE Sensors Journal, 2017, 17, 6268-6278.	4.7	7

GUANG-CAI SUN

3

#	Article	IF	CITATIONS
55	Focusing of MEO SAR Data Based on Principle of Optimal Imaging Coordinate System. IEEE Transactions on Geoscience and Remote Sensing, 2020, 58, 5477-5489.	6.3	7
56	A Novel Two-Step Scheme Based on Joint GO-DPCA and Local STAP in Image Domain for Multichannel SAR-GMTI. IEEE Journal of Selected Topics in Applied Earth Observations and Remote Sensing, 2021, 14, 8259-8272.	4.9	7
57	Refocusing of Moving Ships in Squint SAR Images Based on Spectrum Orthogonalization. Remote Sensing, 2021, 13, 2807.	4.0	7
58	A Real-Time Imaging Processing Method Based on Modified RMA with Sub-Aperture Images Fusion for Spaceborne Spotlight SAR. , 2020, , .		7
59	A Multi-Perspective 3D Reconstruction Method with Single Perspective Instantaneous Target Attitude Estimation. Remote Sensing, 2019, 11, 1277.	4.0	6
60	Time-Varying Baseline Error Estimation and Compensation in UAV SAR Interferometry Based on Time-Domain Subaperture of Raw Radar Data. IEEE Sensors Journal, 2020, 20, 12203-12216.	4.7	6
61	Focusing Challenges of Ships With Oscillatory Motions and Long Coherent Processing Interval. IEEE Transactions on Geoscience and Remote Sensing, 2021, 59, 6562-6572.	6.3	6
62	A High-Resolution and High-Precision Passive Positioning System Based on Synthetic Aperture Technique. IEEE Transactions on Geoscience and Remote Sensing, 2022, 60, 1-13.	6.3	6
63	A new signal model for a wideband synthetic aperture imaging sensor. Canadian Journal of Remote Sensing, 2011, 37, 171-183.	2.4	5
64	A New Method to Obtain 3-D Surface Deformations From InSAR and GNSS Data With Genetic Algorithm and Support Vector Machine. IEEE Geoscience and Remote Sensing Letters, 2022, 19, 1-5.	3.1	5
65	2-D Beam Steering Method for Squinted High-Orbit SAR Imaging. IEEE Transactions on Geoscience and Remote Sensing, 2021, 59, 4827-4840.	6.3	5
66	A Real-Time Unified Focusing Algorithm (RT-UFA) for Multi-Mode SAR via Azimuth Sub-Aperture Complex-Valued Image Combining and Scaling. IEEE Transactions on Geoscience and Remote Sensing, 2022, 60, 1-17.	6.3	5
67	A Postmatched-Filtering Image-Domain Subspace Method for Channel Mismatch Estimation of Multiple Azimuth Channels SAR. IEEE Transactions on Geoscience and Remote Sensing, 2022, 60, 1-14.	6.3	4
68	Moving Target Radial Velocity Estimation Method for HRWS SAR System Based on Subspace Projection. IEEE Geoscience and Remote Sensing Letters, 2022, 19, 1-5.	3.1	4
69	Time-Frequency Reversion-Based Spectrum Analysis Method and Its Applications in Radar Imaging. Remote Sensing, 2021, 13, 600.	4.0	4
70	A Robust Image-Domain Subspace-Based Channel Error Calibration and Postimaging Reconstruction Algorithm for Multiple Azimuth Channels SAR. IEEE Transactions on Geoscience and Remote Sensing, 2022, 60, 1-18.	6.3	4
71	A Novel Multi-Angle SAR Imaging System and Method Based on an Ultrahigh Speed Platform. Sensors, 2019, 19, 1701.	3.8	3

72 Intersatellite cloud computing system for GF-3 SAR data real-time processing. , 2019, , .

GUANG-CAI SUN

#	Article	IF	CITATIONS
73	ISAR Image Matching and Three-Dimensional Scattering Imaging Based on Extracted Dominant Scatterers. Remote Sensing, 2020, 12, 2699.	4.0	3
74	A Modified Range Model and Doppler Resampling Based Imaging Algorithm for High Squint SAR on Maneuvering Platforms. IEEE Geoscience and Remote Sensing Letters, 2020, 17, 1923-1927.	3.1	3
75	Multiple Statistics Contributing to Few-Sample Deep Learning for Subtle Trace Detection in High-Resolution SAR Images. IEEE Transactions on Geoscience and Remote Sensing, 2022, 60, 1-14.	6.3	3
76	High squint multichannel SAR imaging algorithm for high speed maneuvering platforms with small-aperture. Signal Processing, 2021, 185, 108078.	3.7	3
77	Azimuth Variant Motion Error Compensation Algorithm for Airborne SAR Imaging Based on Doppler Adjustment. IEEE Geoscience and Remote Sensing Letters, 2022, 19, 1-5.	3.1	3
78	High-Speed Maneuvering Platform SAR Imaging With Optimal Beam Steering Control. IEEE Transactions on Geoscience and Remote Sensing, 2022, 60, 1-12.	6.3	3
79	Attributed Scattering Center Extraction Method for Microwave Photonic Signals Using DSM-PMM-Regularized Optimization. IEEE Transactions on Geoscience and Remote Sensing, 2022, 60, 1-16.	6.3	3
80	Factorised polarâ€format backâ€projection algorithm. IET Radar, Sonar and Navigation, 2015, 9, 875-880.	1.8	2
81	SAR Ground Maneuvering Targets Imaging and Motion Parameters Estimation Based on the Adaptive Polynomial Fourier Transform. IEEE Geoscience and Remote Sensing Letters, 2022, 19, 1-5.	3.1	2
82	High Speed Maneuvering Platform Squint TOPS SAR Imaging Based on Local Polar Coordinate and Angular Division. Remote Sensing, 2021, 13, 3329.	4.0	1
83	Azimuth Spectrum Reconstruction Algorithm for Multichannel Squint Sar on High Speed Airborne Platform. , 2021, , .		1
84	An Efficient MEO SAR Imaging Algorithm Based on Optimal Imaging Coordinate System. , 2020, , .		1
85	Long Synthetic Aperture Passive Localization Using Azimuth Chirp-Rate Contour Map. , 2020, , .		1
86	Unambiguous Signal Reconstruction Algorithm for High Squint Multichannel SAR Mounted on High Speed Maneuvering Platforms. , 2020, , .		1
87	Ship Focusing and Positioning Based on 2-D Ambiguity Resolving for Single-Channel SAR Mounted on High-Speed Maneuvering Platforms With Small Aperture. IEEE Transactions on Geoscience and Remote Sensing, 2022, 60, 1-13.	6.3	1
88	Applications of Baseband Azimuth Scaling on High Squint Beam Steering SAR Imaging with Contant Acceleration. , 2019, , .		0
89	A New Approach for Optimization Selection of Spaceborne SAR Beam Position Parameters. , 2019, , .		0
90	Ship Imaging based on Azimuth Ambiguity Resolving for High-Speed Maneuvering Platforms Sar with Small-Aperture. , 2021, , .		0

#	Article	IF	CITATIONS
91	Design of Double-Mode Integrated Microwave Remote Sensor for Ocean Wave Observation. , 2021, , .		Ο
92	Fast Rotation Matching Method for SAR and Optical Images. IEEE Journal of Selected Topics in Applied Earth Observations and Remote Sensing, 2021, , 1-1.	4.9	0